EUROPEAN ORGANIZATION FOR NUCLEAR RESEARCH
Laboratory for Particle Physics

Divisional Report

CERN LHC/2000-6   (MTA)

Validation of a Computer Code for Use in the Mechanical Design of Spallation Neutron Targets

Paul A. Montanez[1] and Peter Sievers[2]

The present work concentrates on comparing a numerical code and a closed-form analytic solution for determining transient stress waves generated by an impinging, high-intensity proton pulse onto a perfectly elastic solid cylindrical target. The comparison of the two methods serves both to benchmark the physics and numerical methods of the codes, and to verify them against analytic expressions that can be established for calculating the response of the target for simple cases of loading and geometry. Additionally, the comparison elucidated the effects of approximations used in the computation of the analytic results. Two load cases have been investigated: (1) an instantaneously uniform thermal loading along the central core, and (2) a ramped and uniform thermal load applied along the central core. In addition, the influence of the approximations applied to the accurate analytic forms has been elucidated. By validating these analytical results, the closed-form solution may be confidently used to "bound" the solution prior to initiating more detailed and comprehensive numerical studies.

1 National Synchrotron Light Source, Brookhaven National Laboratory, Building 725D, Upton NY 11973, USA
2 CERN - European Organization for Nuclear Research, LHC Division, CH - 1211 Geneva 23, Switzerland

Administrative Secretariat
LHC Division
CERN
CH - 1211 Geneva 23

Geneva, Switzerland
6 November 2000

INTRODUCTION

This work documents the use of the LS-DYNA® [1, 2] finite element code to benchmark a series of analytic expressions used in determining the stress distribution in solid, high density targets which are thermally loaded by high-intensity proton beams. These targets are a critical sub-component of state-of -the-art spallation neutron sources that provide neutron beams for the study of the structure and dynamics of materials. Conventional target designs use high-density metal plates separated by water-cooling. Concepts using liquid heavy metals have been adopted to increase neutron production by making the target and coolant one and the same. An alternative to the conventional plate design is an edge-cooled design, which provides a target of pure heavy metal but does not require a circulating liquid metal for cooling. Such a design would increase the brightness of the neutron source (which increases the intensity of the source) for the users. It is this edge-cooled design that we ultimately hope to accurately model using the results of this benchmark.

A solid rod spallation neutron production target, based on the anti-proton target developed at CERN [3,4], is composed of essentially three components. At the core of the target is a solid cylinder of high-density material, typically Tungsten or Iridium. The choice of a high-density target material allows for copious production of neutrons. Surrounding the target core is a hollow cylinder of graphite which acts primarily to evacuate the heat, by radiation and conduction through the air/gas gap and via chaotic contact points, to the third component, a thin-walled containment shell, possibly an aluminum or titanium alloy. This sub-assembly is contained within another shell between which coolant flows to remove the heat generated from the energy transfer from the proton beam to the target core material.

This numerical study will concentrate primarily on the transient dynamic response of a perfectly elastic rod due to cylindrical stress waves generated by a uniformly applied thermal loading and originating in the center of a cylinder. These stress waves were studied by Sievers [5] using a Fourier-Bessel series.

Prior to initiating a detailed computational study of the transient dynamic response of an edge-cooled, multi-material production target, a numerical study should be

undertaken to ensure that the code is a good predictor of the physical phenomena expected in such a device. There are many complex nonlinear phenomena involved in simulating the response of the proposed composite neutron production target. These are typically in the form of contact, plasticity, material failure, and quite possibly large deformation effects of the individual materials composing the target. Although these nonlinearities are not addressed in the present study, it is understood that if the code can accurately represent the physics of the thermo-elastic model at hand, the addition of more complex constitutive relations and other nonlinearities should not hinder the ability of the code to accurately simulate these details as well.

LS-DYNA® is a large, general purpose, explicit code which contains many user options from which to choose to accurately simulate nonlinear phenomena and to adjust parameters such as hourglass control, bulk viscosity, damping, and time step size, to name just a few. A baseline study of a radially and axially constrained solid cylinder (Figure 1) will serve to identify and define which analysis options should be employed in solving this particular class of hyperbolic partial differential equations (P.D.E.). Since the primary element formulations used by LS-DYNA® employ one-point integration, "hourglassing" might be of some concern and is studied here. An artificial bulk viscosity approach is used in LS-DYNA® to treat shock waves by adding a "viscous" term to the pressure to smear shock discontinuities, this might also be of some concern if large enough proton energies are absorbed which give rise to shock waves. The range of acceptable values for bulk viscosity will also be studied.

BACKGROUND

Analytic Solution

Analytic solutions are derived in a classical way by Sievers[5], based on principles of acoustic waves in linear, elastic matter, for longitudinally and radially constrained cylinders. A more comprehensive assessment, including radially free solids and liquids is in preparation [6] where some flaws contained in the earlier paper [5] are also corrected.

The equation of motion for a cylindrical body is described by,

$$\frac{\partial^2 U}{\partial r^2} + \frac{1}{r}\frac{\partial U}{\partial r} - \frac{U}{r^2} = \frac{1}{c}\frac{\partial^2 U}{\partial t^2} \tag{1}$$

subject to the boundary and initial conditions

$$U(0,t) = U(R,t) = 0 \text{ and } U(r,0) = -\overline{U}(r) \tag{2}$$

where $\overline{U}(r)$ are the static displacements and the assumed temperature distribution is described by,

$$T(r) = \begin{cases} T_0 & 0 \le r \le r_0 \\ 0 & r_0 \le r \le R \end{cases} \tag{3}$$

Solving the differential equation according to these conditions yields, for the *radial* component of dynamic stress [5]:

$$\sigma_{0,r}(r,t) = \frac{2E\alpha T_0}{(1-2\upsilon)}\sum_{n=1}^{\infty}\xi_0 \frac{J_1(z_{0,n}\xi_0)}{J_0^2(z_{0,n})z_{0,n}}\left[J_0(z_{0,n}\xi) - \frac{(1-2\upsilon)}{(1-\upsilon)}\frac{J_1(z_{0,n}\xi)}{z_{0,n}\xi}\right]cos(z_{0,n}\Theta) \tag{4}$$

where we have

$$\xi_0 = \frac{r_0}{R}, \qquad \xi = \frac{r}{R}, \qquad and \qquad \Theta = \frac{ct}{R}$$

and the sound velocity is given by:

$$c = \sqrt{\frac{E(1-\upsilon)}{\rho(1+\upsilon)(1-2\upsilon)}}$$

The radial "quasi-static", thermal stress component is described by:

$$\overline{\sigma}_r = \begin{cases} \dfrac{E\alpha T_0}{2(1-\upsilon)}\left[1 + \dfrac{r_0^2}{R^2}\dfrac{1}{(1-2\upsilon)}\right] & 0 \le r \le r_0 \\ \dfrac{E\alpha T_0}{2(1-\upsilon)}\left[\dfrac{r_0^2}{r^2} + \dfrac{r_0^2}{R^2}\dfrac{1}{(1-2\upsilon)}\right] & r_0 \le r \le R \end{cases} \tag{5}$$

Here, E is the elastic modulus, α is the coefficient of thermal expansion and υ is Poisson's ratio. The "total" stress (dynamic + quasi-static) is obtained by superposing Eqn's 4 and 5 and evaluating them numerically using the Mathematica® [7] program. In the dynamic stress (Eq. 4), $z_{0,n}$ represents the zeros of the first order Bessel function. An approximation to these zeros is given as:

$$z_{0,n} = \pi(n + \frac{1}{4}) \tag{6}$$

The total stress computed using this approximation to the zeros as well as the "exact" roots, as computed by the Mathematica® root finding algorithm, will be compared.

It can readily be shown [6] that for rapid heating at time zero all principle components of the total stress are equal and have a value:

$$\frac{E\alpha T(r)}{1-2\mu} \tag{7}$$

A more representative finite pulse can readily be derived by folding the instantaneous solution with the rise of the pulse by solving the convolution integral, as indicated in [5]. For this case, Eq. (4) must be scaled by the factor $\frac{1}{\Theta_0}$, where $\Theta_0 = \frac{ct_0}{R}$, and the cos(*) term must be replaced with:

$$\cos(*) \Rightarrow \begin{cases} \dfrac{\sin(z_{0,n}\Theta)}{z_{0,n}} & 0 \le t \le t_0 \\ \dfrac{\sin(z_{0,n}\Theta) - \sin[z_{0,n}(\Theta - \Theta_0)]}{z_{0,n}} & t_0 < t \end{cases} \tag{8}$$

where t_0 is the pulse length.

Similar expressions have been derived for the hoop (tangential) and axial components and may be found in [5].

The derivation given in [5] for the stress components ignores the effects of thermal conduction. This is a reasonable assumption where the loading is applied over a time scale of microseconds, as in the case of high-intensity proton accelerators, since the Fourier modulus is very much less than unity. The dimensionless Fourier modulus compares a characteristic body dimension, in this case the radius of the rod, with an approximate temperature-wave penetration depth for a given time. For our particular material, geometry, and analysis period (50μs), this Fourier modulus is on the order of 10^{-4}.

One note of caution, the stress components in [5] carry a sign convention which is opposite of that traditionally defined in solid mechanics texts and that which is employed in most commercial Finite Element codes so the analytic results must be adjusted to compare with the numerical work.

Computational Solution

LS-DYNA® is a general-purpose explicit finite element program [1, 2] used to analyze the nonlinear, transient dynamic response of three-dimensional solids and structures. As an explicit code, LS-DYNA® is appropriate for problems where high rate dynamics or stress wave propagation effects are important. In contrast to an implicit code, LS-DYNA® does not form and solve the large matrix equation typical of an implicit code and does not require iteration at each time step.

LS-DYNA® is based on a finite element discretization of the three spatial dimensions and a finite difference discretization of time. The explicit central difference method is used to integrate the equations of motion in time. The central difference method is conditionally stable, with stability governed by the Courant limit on the time step, Δt. For solid elements, this limit is essentially the time required for an elastic stress wave to propagate across the shortest dimension of the smallest element in the mesh. Equivalently, this maximum time step may be related to the period of the highest free vibration mode of the finite element mesh. LS-DYNA® automatically calculates the maximum time step size at each step of the solution, thus minimizing the cost of the analysis while ensuring that stability is maintained.

LS-DYNA® uses a lumped mass formulation for efficiency. This produces a diagonal matrix, M, which renders the solution of the momentum equation

$$M\mathbf{a}_{n+1} = \mathbf{f}^{ext} - \mathbf{f}^{int} \tag{9}$$

trivial at each step in that no simultaneous system of equations must be solved. In the above equation, f^{ext} are the applied external forces, and f^{int} are the element internal forces. The new accelerations a_{n+1} are easily found, from which the updated velocity and coordinates are calculated using the central difference integration formulas. In LS-DYNA® the initial conditions to the transient dynamic problem are specified as initial velocities. Boundary conditions of many types ranging from constrained nodal translations and rotations to nonreflecting boundaries are easily prescribed.

In an explicit code there are many small time steps so it is important to minimize the number of operations performed at each time step. This minimization is accomplished by using elements with one-point Gauss quadrature for the element

integration. This formulation leads to spurious zero energy deformation modes, the so-called "hourglass modes", within the element. Using an "hourglass viscosity" or "hourglass stiffness" while retaining legitimate deformation modes stabilizes these spurious modes.

DISCUSSION

Idealization of Problem and LS-DYNA Options

All calculations were made on a Sun Microsystems® Ultra60 running the Solaris2.7 OS with a single 360-MHz UltraSparc-II processor and 1GB of RAM. Mesh generation is provided externally to the LS-DYNA® code by using the commercially available pre-processing package TrueGrid® [8]. The finite element discretization of a solid iridium rod of arbitrary length, outer radius of 0.5cm, and "heated region" of radius R/2 (0.25cm), is accomplished by recognizing that taking advantage of symmetry conditions may reduce the computational model significantly. The so-called "heated region" is that volume of the cylinder that is intercepted by the impinging proton beam. A quarter symmetry model with the appropriate boundary conditions and heated region is given in Figure 1 for visualization.

Prior to constructing the mesh we observe that the geometry, material properties and loading of the cylindrical target are axisymmetric. The symmetry allows us to implement a 2-dimensional representation of the physically 3-dimensional object. Except for the need to account for circumferential strain, ε_θ, axisymmetric elements are very similar to plane elements. Though the element is geometrically two-dimensional, the stress tensor is composed of the nonzero components $\sigma = \{\sigma_r, \sigma_\theta, \sigma_z, \tau_{zr}\}$ where the global finite element Cartesian coordinate system is related to the cylindrical system by $(X,Y,Z) = (r,z,\theta)$. By virtue of the fact that 2D elements require fewer computational resources per element than their 3D counterparts, many more degrees-of-freedom may be modeled resulting in an increased accuracy of the resulting stress tensor. While this limit on computational resources may not be relevant in the present study, subsequent modeling of the full composite target assembly may require the addition of some or all of the following: non-axisymmetric geometry/loading, material/geometric nonlinearities and contact conditions one or all

of which may dictate that we extend our 2-dimensional approach to the full 3D space. However, it is important to verify that a 2D axisymmetric approach gives valid results since LS-DYNA® already has many of the previously mentioned nonlinear options implemented as 2-dimensional features which may still allow the more complex simulation to be run as an axisymmetric model.

A second resource-conserving observation is that the analytic expressions for the stress components are one-dimensional, i.e., they have only a radial dependence; a one-element thick "disk" (in the axial direction) can be constructed to represent the target rather than meshing the full length of the target, see Figure 2.

Finally, by choosing this 2D representation, we are able to get a much more rapid turn around time for the various parametric studies that we wish to undertake in our benchmark study to gain insight into the physical behavior of a solid spallation target.

The cross section of the axisymmetric model was meshed with unit aspect ratio, quadrilateral, 2D-axisymmetric, Petrov-Galerkin (area weighted), one-point integration elements. There are two displacement degrees-of-freedom, {u,v}, per node. It is worth stating that in this axisymmetric configuration the global Y-axis must be the axis of symmetry and the X-axis therefore corresponds to the radial direction. The boundary conditions are satisfied by setting the radial displacement, u (=dx), for all nodes at r=0 and r=R to zero and v (=dy)=0 for all nodes at either axial boundary of the mesh. Applying a zero initial velocity to all nodes satisfies the initial condition.

Boundary conditions and material properties are specified through TrueGrid® commands and written to the LS-DYNA® keyword format input deck. LS-DYNA® employs a comprehensive library of constitutive relations available for modeling various types of material behavior such as plastics, metals composites, soils etc. For our simulation, the ***MAT_ELASTIC_PLASTIC_THERMAL** (Material Type 4) model was chosen to model an isotropic, ideally elastic material. This material model allows for the defining of temperature dependent material coefficients in a thermo-elastic-plastic material (see Table I for input values [9, 10]). Although this constitutive model is capable of simulating the effects of inelasticity, we are interested

in modeling only the <u>thermo-elastic</u> behavior of the target to compare with the analytic solution in [5]. To simulate this constitutive behavior, the yield stress is set to a large number (on the order of the Elastic Modulus) to ensure that there is no plastic flow, i.e. perfectly elastic material behavior. Likewise the tangent modulus, E_t, was set to zero.

In the case of the instantaneously heated rod, a uniform thermal load of 890°C, which is an equivalent energy of 30 kJ, is applied to all nodes of the elements comprising the heated region (see the cross hatched region in Figures 1 and 2) through the ***LOAD_THERMAL_CONSTANT** command for the entire length of the analysis. For the finite length pulse calculations the LS-DYNA® keyword command ***LOAD_THERMAL_VARIABLE** was used in conjunction with the ***DEFINE_CURVE** command to ramp the thermal loading from zero to a constant value over a period of 0.15 μs (the length of the proton pulse from the BNL AGS storage ring) and then held constant for the remainder of the analysis. Use of the ***LOAD_THERMAL_***OPTION* family of commands ignore thermal conduction. This is rather fortuitous since this is exactly the behavior that we are trying to simulate, i.e. the analysis period is of sufficiently short duration that heat transfer due to conduction is negligible. This family of commands provides for the load application by allowing for a temperature state to be read in and held constant throughout the analysis, thereby dynamically loading the structure. This method of loading the model assumes that thermal conduction is negligible throughout the analysis period and is consistent with the assumption in [5]. One particularly advantageous feature of this method of loading the structure is that a sequentially-coupled or fully-coupled thermo-elastic analysis is bypassed, i.e. an independent thermal analysis to calculate the loading to be applied for the transient dynamic analysis prior to initiating the dynamic analysis is not required.

A time step scale factor (TSSFAC field on the ***CONTROL_TIMESTEP** card) was set to 1. Choosing this value ensures that the Courant time step is used in the transient calculations, thereby helping to ensure that any numerical dispersion is minimized. Various LS-DYNA® user options were adjusted to determine the optimum code settings for obtaining a valid numerical solution for a particular class of problems encountered in the design of neutron spallation facilities. Foremost among those user

options studied include: bulk viscosity coefficients
(***CONTROL_BULK_VISCOSITY**) and hourglass coefficient
(***CONTROL_HOURGLASS**) effects, time step scaling factor
(***CONTROL_TIMESTEP**), number of element integration points
(***SECTION_SHELL**, NIP field) and element formulation (***SECTION_SHELL**,
ELFORM field).

RESULTS

A numerical comparison was made between LS-DYNA element types 14 (Petrov-Galerkin area weighted) and 15 (Galerkin volume weighted) which produced consistent results for this benchmark case. These two element types are of such different formulation so as to represent two independent solutions and their similar results help to form a basis for our confidence in the computed results of the code.

The LS-DYNA® default values for bulk viscosity coefficients and viscosity formulation were found to be satisfactory; an order of magnitude increase in the bulk viscosity did not enhance the results noticeably. Default hourglass viscosity type and coefficient were likewise found to be adequate with the default one-point integration elements. Performing an analysis with fully integrated elements (NIP=4) produced no discernible differences in the finite element solution results; therefore one-point integration elements will be defined in all LS-DYNA® keyword input decks in these studies. Should an unacceptable level of hourglass energy in the computational results be observed, the analyst should consider using fully integrated elements rather than the one-point integration elements, though this may dramatically increase the run times of any analysis. One-point integration elements should be used in simulating any detailed target assembly since material nonlinearities and contact will be included. By using the default one-point integration element, the problem becomes more tractable from a computational point of view.

Finite element solutions to the transient dynamic problem were calculated with several mesh densities. In particular, computational meshes with 100, 200, 500 and 1000 elements were generated. In all cases the computational domains were

constructed so as to be composed of elements which all have unit aspect ratio. It was determined, by comparing the stress components σ_x, σ_y and σ_z in successive solutions, that a mesh with 500 elements in the radial direction gave results that did not differ significantly from the result set obtained from a model with 1000 elements. This 500-element model also had run times that were of manageable duration for the numerous parametric studies undertaken here. In all of the plots for σ_{TOTAL}, which compare the analytic and computational radial component of total stress, the finite element results were extracted at the centroid of the second element from the centerline, at a radial location of 0.0015cm.

In the process of comparing the results obtained from the analytic and numerical work, it was found that the approximation to the zeros of the first order Bessel function (Eq. 6) is of limited validity for the solution of the analytic stress components. While Figure 3 shows that the greatest difference between the approximate and exact zeros is on the order of 2.5% in the first root and decreasing thereafter, this discrepancy propagates itself through the dynamic stress component, resulting in erroneous results after the first few microseconds, or periods, of the result for the total stress. Using Eq. 6 as an approximation to the zeros, and combining the radial quasi-static (Eq. 5) and dynamic components to compute the total radial stress, yields the results given in Figure 4. A more correct result is obtained for the dynamic (and total) stress when the exact zeros are employed, as is seen in Figure 5. Having determined that Eq. 6 is not precise enough for our numerical work, all subsequent evaluations of the dynamic stress components are calculated with the exact roots to the first order Bessel function.

In calculating the analytic solution, it was found that retaining 500 terms of the infinite series for the dynamic stress component was sufficient to accurately calculate the response of each component of the stress tensor, i.e., radial, axial and tangential (hoop). Retaining fewer terms than this resulted in excessive numerical noise in the time history plots, particularly in the case of the instantaneously applied thermal load. For the solution to the case of a ramped load, fewer terms were required to obtain a smoothly varying curve; however, to maintain consistency in the approach taken for comparing solutions the same number of terms used in the solution of the dynamic stress component was retained as in the case of an instantaneously loaded body.

The origin of the sharp spikes that are seen in the analytic result for instantaneous loading but not in the numerical solution, Figures 6-8, was investigated. A sensitivity study of (1) the total number of terms retained in the solution of the dynamic component of total stress and (2) the time step, were performed. As seen in Figure 9, with a constant time increment of 0.01, the sharp spikes in the solution for the total stress are essentially unaffected by retaining an ever-greater number of terms for the dynamic radial stress component of the total stress. If we also plot the sensitivity of the total radial stress to the time step, Figures 10 and 11, we find that the peaks grow larger for smaller time steps as we would expect up to a limit. This shows that the analytic solution is rather robust in that the peaks do not continue to grow unbounded for a corresponding decrease in the time step. The most likely origin of these sharp spikes is due to the sharp step in the temperature distribution described by Eq. 3. For the finite element solution, the numerical methods employed in the time integration algorithm tend to "smear-out" the sharp spikes due to their finite time-step size. It has been shown in [6] that by employing a parabolic temperature profile rather than a step-function distribution results in continuously smooth results for the solution to the analytic equations.

 A more telling result in attempting to cross correlate the analytic and numerical solutions is given by the results obtained for the more physically realistic case of a ramped thermal loading. For this load case, Figures 12-14 show that the correlation is excellent. For most of the analysis period of 50 • s, the results of the analytic and computational are in outstanding agreement. Only after many periods of the stress wave do we notice even a minor disagreement. Figure 13 indicates that there are some larger radial stresses predicted by the analytic expression and Figure 14 shows a slight phase difference of fractions of a microsecond. These discrepancies may be attributed to some slight numerical dissipation or may even be explained by a difference in time step used in the two solutions.

CONCLUSIONS

We have attempted in this paper to verify the applicability of and to provide a framework for using a commercially available finite element code, namely LS-DYNA®, to calculate the stress tensor, and by extension other quantities of engineering importance such as the von Mises equivalent stress, in the evaluation of baseline designs for high energy spallation targets.

It was determined through comparison of analytic and computational results that the roots of the Bessel function J1, as given by Eq. 6, is a relatively poor approximation for use with numerical evaluation of the dynamic component of total stress. We have found that it is critical to use the "exact" zeros found by a root-finding algorithm when the analytic stress components are evaluated in order to obtain accurate estimations for the stress components.

Using the exact zeros it was found that excellent correlation exists between numerical and analytic solutions when calculating the stress tensor for the case of a ramped thermal load on a cylindrical rod target. It was also determined that good correlation between result sets exist for the case of an instantaneously applied thermal load to the rod target, although this type of analysis has its practical limitations due to the nonphysical nature of a step function loading.

We believe that this study shows that the analytic solution can be used as an upper bound for estimating transient loading in problems with similar boundary conditions and may find usefulness as a guide to design choices prior to initiating detailed numerical analysis. Also, it has been determined that a numerical code such as LS-DYNA® may confidently be used to calculate engineering quantities of interest for numerical models containing simple material models and by extrapolation, complex nonlinear phenomena such as contact and inelastic material models.

ACKNOWLEDGEMENTS

REFERENCES

(1)   *LS-DYNA® Keyword Users Manual, Version 950*, Livermore Software Technology Corporation, 1999.

(2)   B.E. Englemann and R.G. Whirley, *DYNA3D A Nonlinear, Explicit, Three-Dimensional Finite Element Code For Solid and Structural Mechanics – User Manual*, Lawrence Livermore National Laboratory, UCRL-MA-107254 Rev. 1, 1993.

(3)   T.W. Eaton, C.D. Johnson, and E. Jones, Recent work on the production of anti-protons from pulsed-current targets, *European Organization for Nuclear Research*, Geneva, Switzerland, CERN/PS/86-15(AA), (July 1994).

(4)   R. Bellone, G. del Torre, M. Ross, P. Sievers, The design and prototype tests of the CERN antiproton production target, *Workshop on High Temperature and Energy Density in Target Materials, Proceedings Univ. Wisc., Madison*, **12**, 48-60 (1981) (CERN SPS 80-9 ABT).

(5)   P. Sievers, Elastic stress waves in matter due to rapid heating by an intense high-energy particle beam, CERN-LAB II/BT/74-2, (1974).

(6)   P. Sievers, *Thermally Induced Stress Waves In Solid And Liquid Cylinders, A Classical Assesment*, CERN, Geneva, Switzerland, In Preparation.

(7)   S. Wolfram, *The Mathematica Book, 3rd Ed.*, Wolfram Media/Cambridge University Press, 1996.

(8)   *TrueGrid® Manual, Version 2.0*, XYZ Scientific Applications Inc., 1999.

(9)   J.R. Davis (Ed.), *Metals Handbook, Desk Edition, 2nd Edition*, American Society for Metals, 1998.

(10)   Y.S. Touloukin, R.K. Kirby, R.E. Taylor, P.D. Desai (Eds.), *Thermophysical Properties of Matter*, IFI/Plenum, New York-Washington, 1973.

FIGURE CAPTIONS

(1)   Quarter symmetry model of the Thermo-Elastic rod model. Shown also are the axial and radial constraints and the heated region.

(2)   Computational domain used for calculating the transient dynamic stress distribution. Cross-hatched area is the "heated region". Shown also are the applied boundary conditions.

(3)   Percent difference between the zeros of Bessel J1 as calculated by Eq. 6 and the "exact" roots that are computed by Mathematica.

(4)   An example of the solution of the radial component of the "total" stress using Eq.6. The loading is an instantaneously applied, uniform thermal load applied to all nodes of the elements comprising the heated region.

(5)   Solution of the radial component of "total" stress using the zeros computed with Mathematica. The loading is the same as that given in Figure 3.

(6)   Comparison of analytic vs. computational results for the radial stress component of a uniformly and instantaneously heated cylindrical rod of radius, R, and heated region, R/2. Five hundred terms of the infinite series for the dynamic component of "total" stress were used in the computation.

(7)   Comparison of the analytic vs. computational radial stress component during the period 20-30 μs for the case of a uniformly and instantaneously heated cylindrical rod.

(8)   Comparison of the analytic vs. computational radial stress component during the period 40-50 μs for the case of a uniformly and instantaneously heated cylindrical rod.

(9)   Parametric study of the number of terms used in the infinite series of the dynamic stress component of the total stress for the analytic solution.

(10)   Parametric study of the time increment, Δt, used in calculating the radial dynamic stress component of total stress for the analytic solution.

(11)   Expanded view of Figure 13 for the time range 0.4-0.58 µs.

(12)   Comparison of analytic vs. computational results for the radial stress
        component of a uniform, ramped thermal loading on a cylindrical rod of
        radius, R, and heated region, R/2. Five hundred terms of the infinite series for
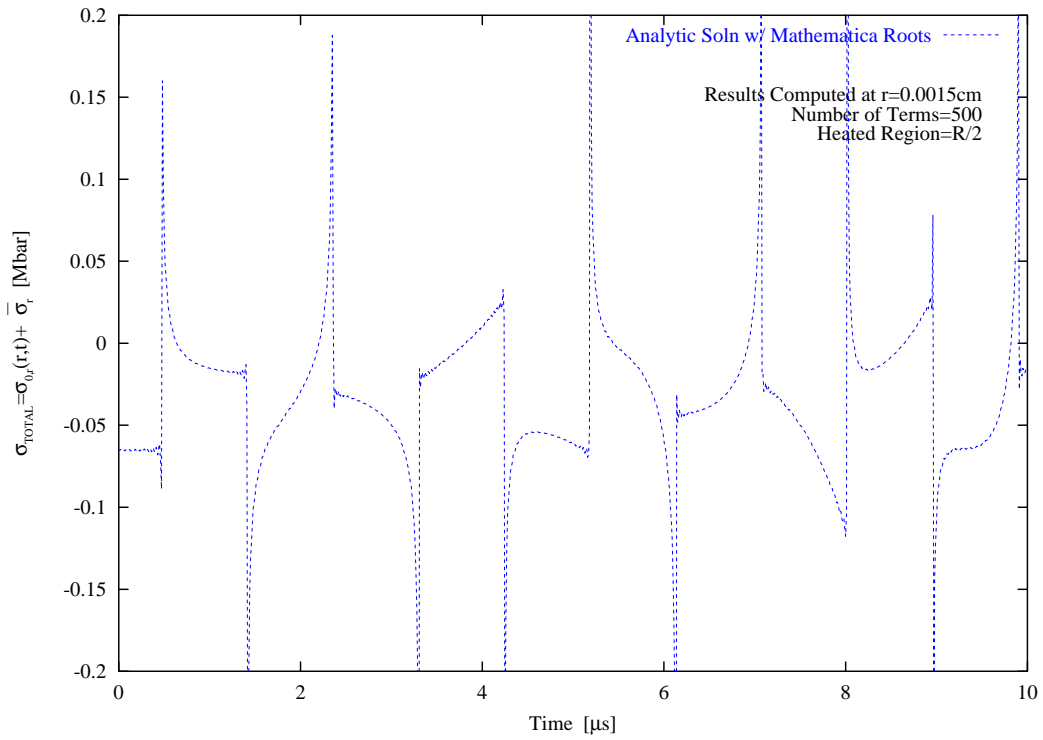   the dynamic component of "total" stress were used in the computation.

(13)   Comparison of radial stress component for the case of a uniform, ramped
        thermal loading over the period 20-30 µs on a cylindrical rod of radius R.

(14)   Comparison of radial stress component for the case of a uniform, ramped
        thermal loading over the period 40-50 µs on a cylindrical rod of radius R.

TABLES AND FIGURES

Table I. Iridium material property values used in analyses.

Material Property	Value	Units
Density, ρ	22.5	g/cm^3
Poisson's Ratio, ν	0.29	
Thermal Expansion Coefficient, α	$6.8 \ 10^{-6}$	cm/cm/°C
Yield Stress, σ_y	10.0	Mbar
Elastic Modulus, E	5.17	Mbar
Tangent Modulus, E_t	0.0	Mbar
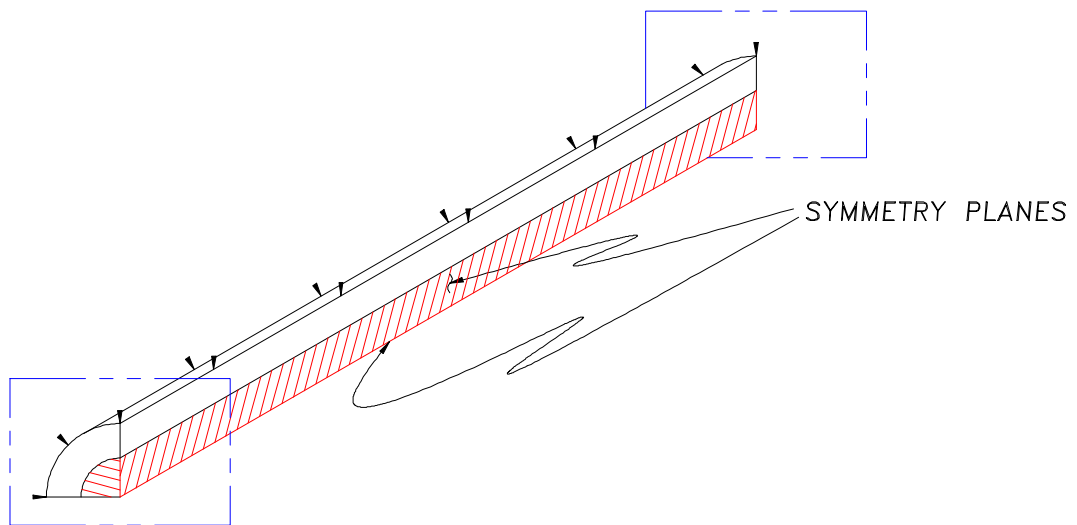
FIGURE 1. Quarter symmetry model of the Thermo-Elastic rod model. Shown also are the axial and radial constraints and the heated region.
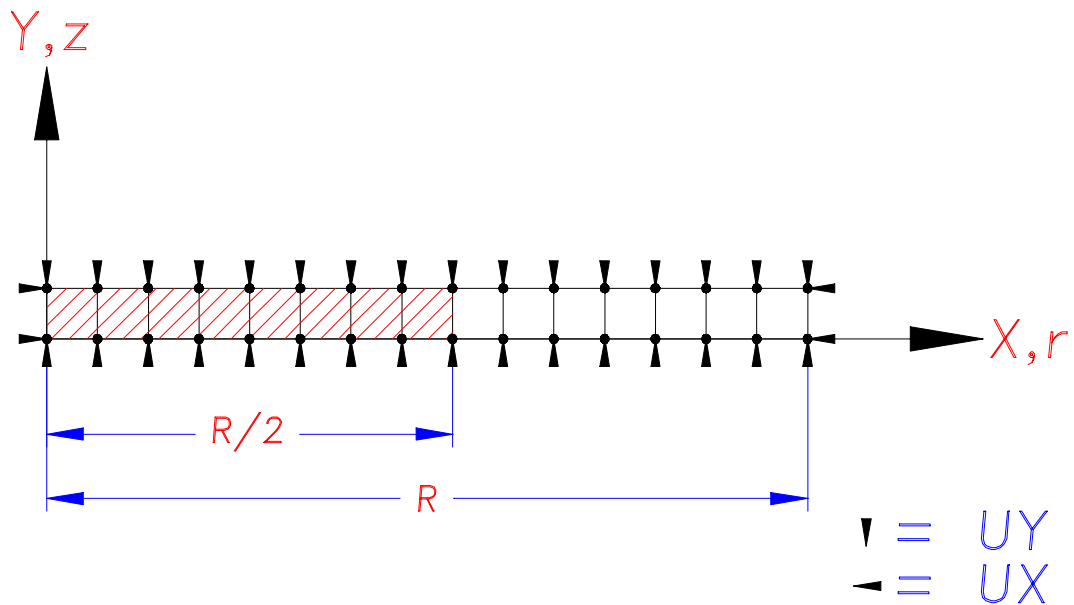
FIGURE 2. Computational domain used for calculating the transient dynamic stress distribution. Cross-hatched area is the "heated region". Shown also are the applied boundary conditions.
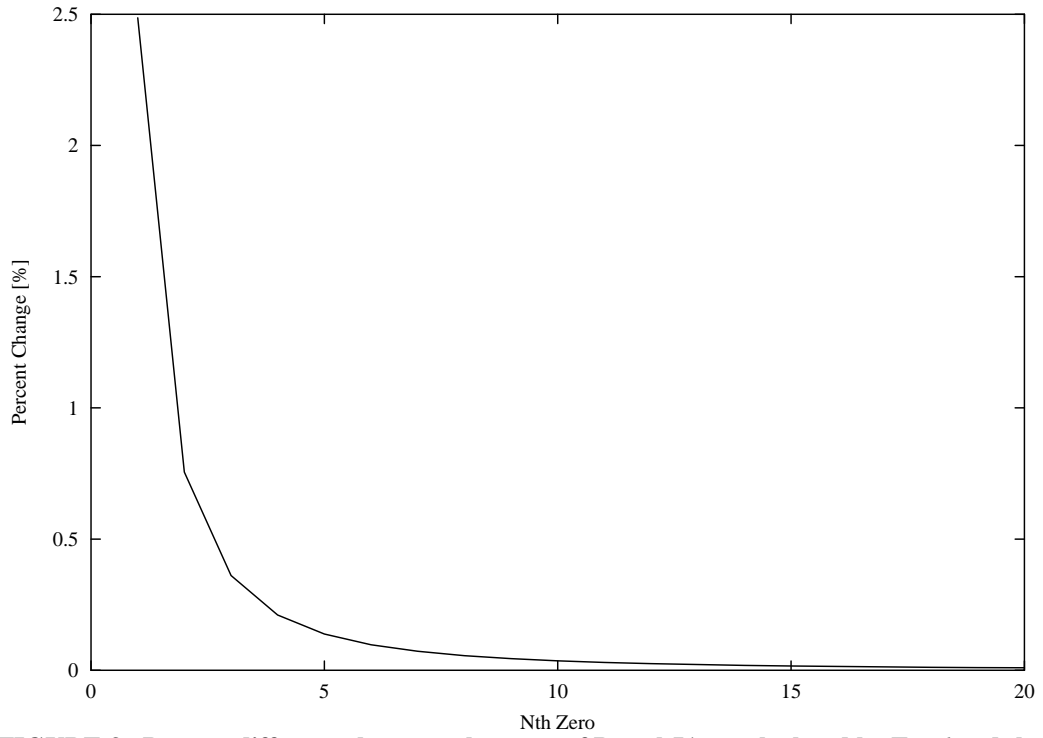
FIGURE 3. Percent difference between the zeros of Bessel J1 as calculated by Eq. 6 and the "exact" roots that are computed by Mathematica.
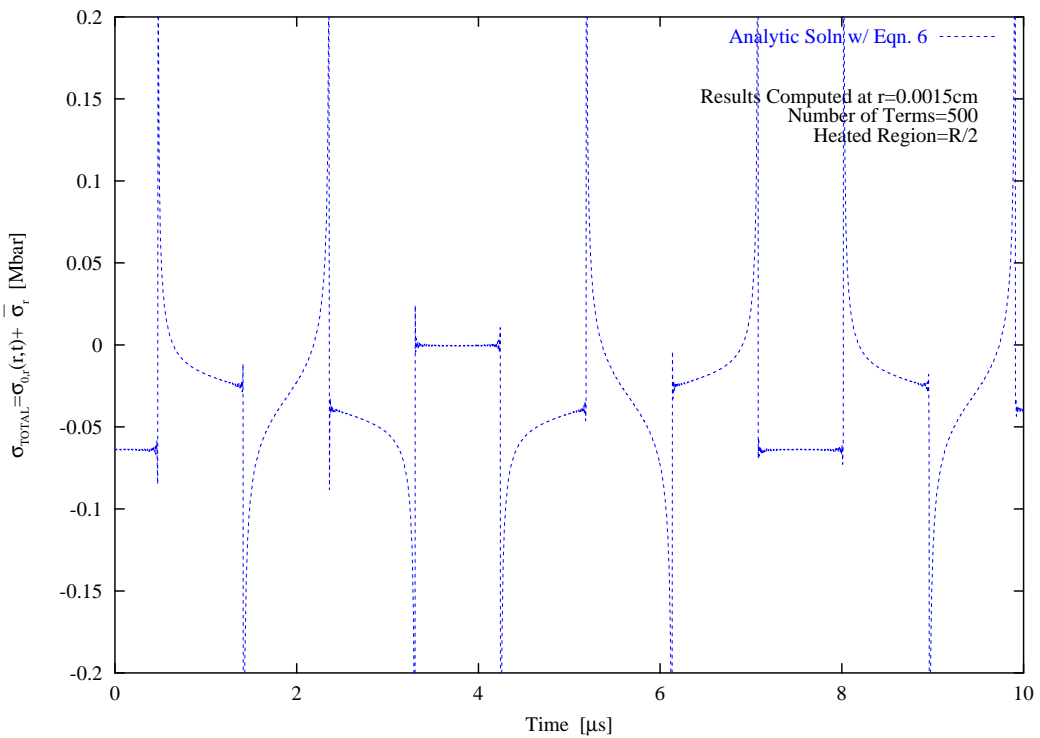
FIGURE 4. An example of the solution of the radial component of the "total" stress using Eq.6. The loading is an instantaneously applied, uniform thermal load applied to all nodes of the elements comprising the heated region.

19

FIGURE 5. Solution of the radial component of "total" stress using the zeros computed with Mathematica. The loading is the same as that given in Figure 3.
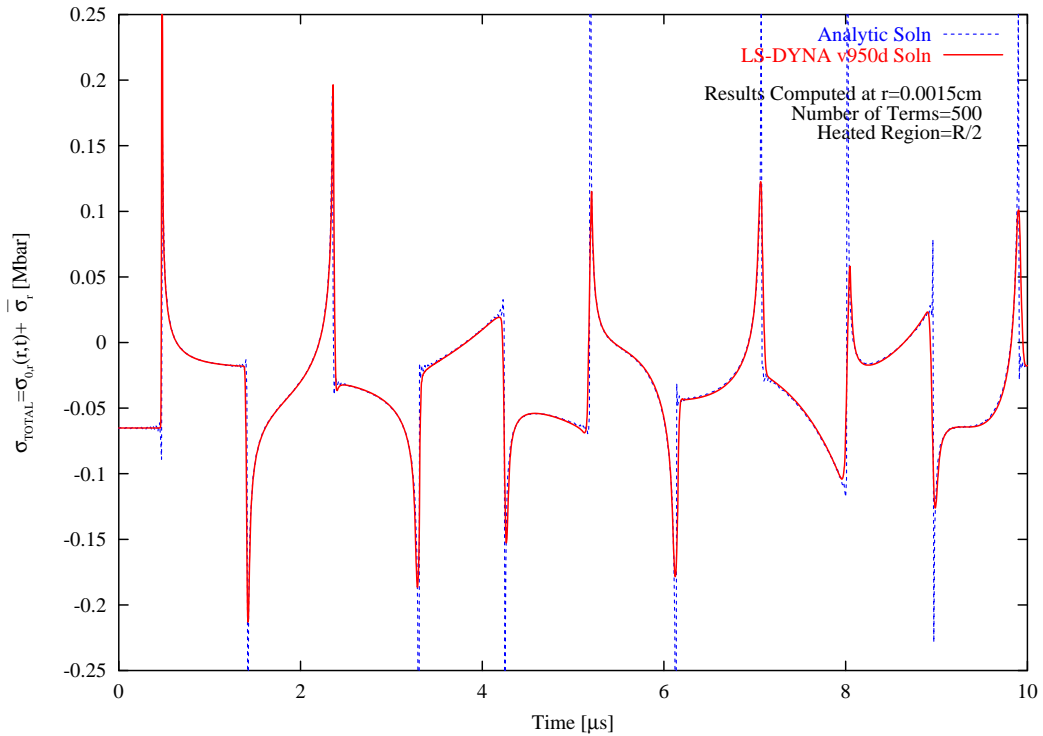
FIGURE 6. Comparison of analytic vs. computational results for the radial stress component of a uniformly and instantaneously heated cylindrical rod of radius, R, and heated region, R/2. Five hundred terms of the infinite series for the dynamic component of "total" stress were used in the computation.
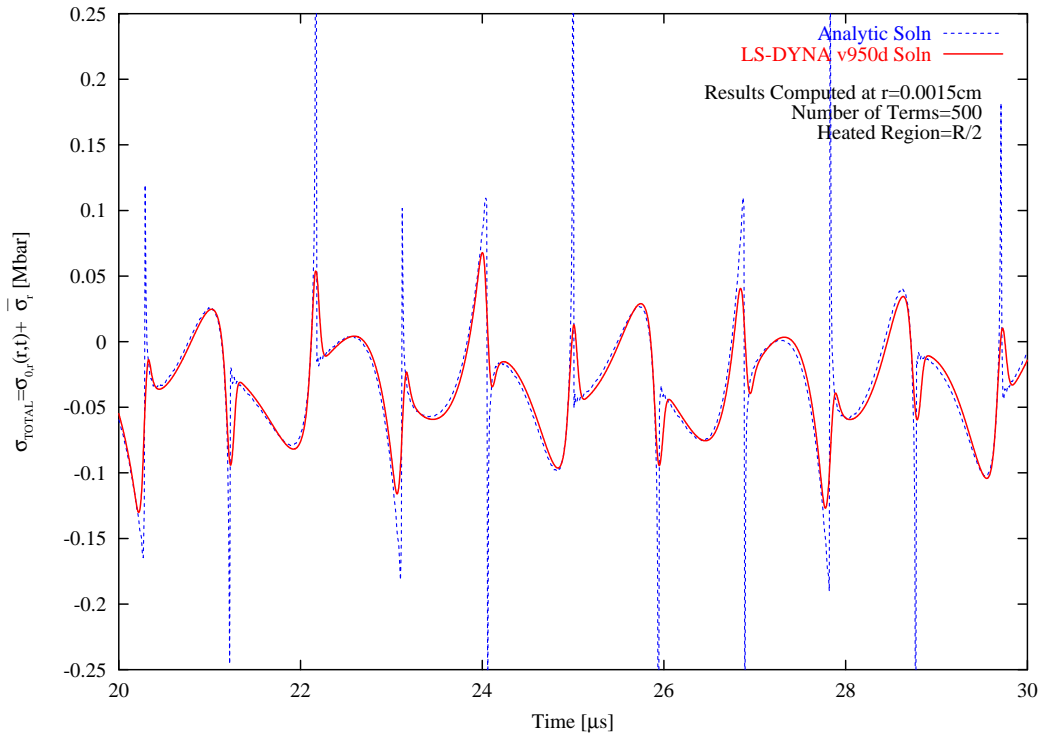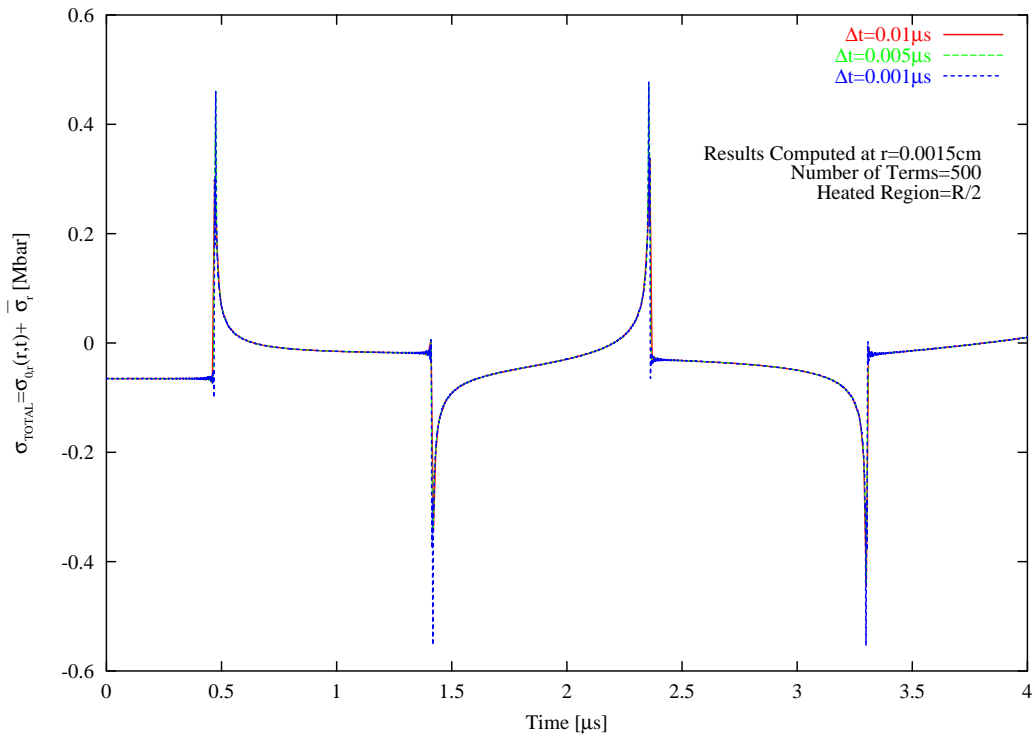
FIGURE 7. Comparison of the analytic vs. computational radial stress component during the period 20-30 μs for the case of a uniformly and instantaneously heated cylindrical rod.
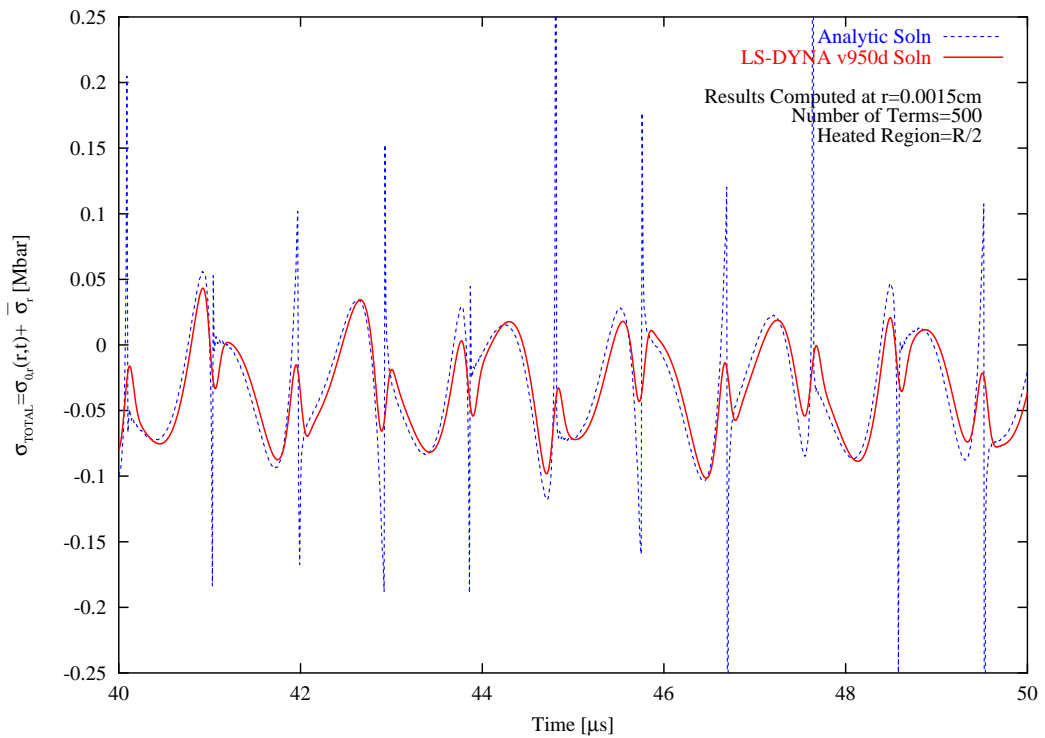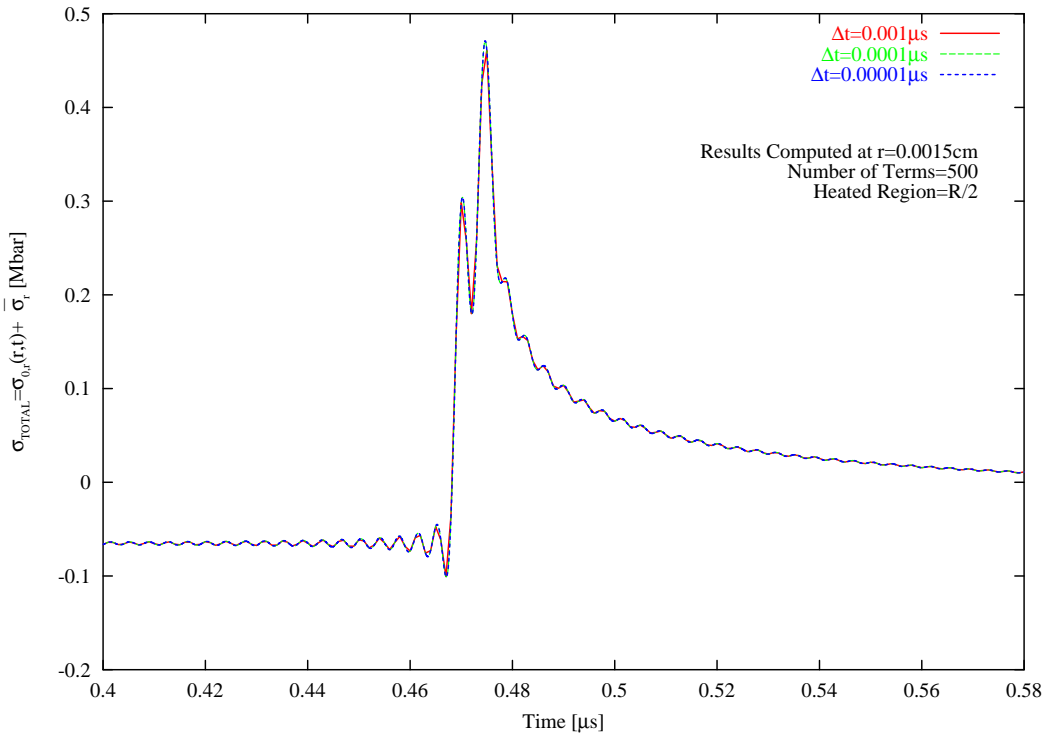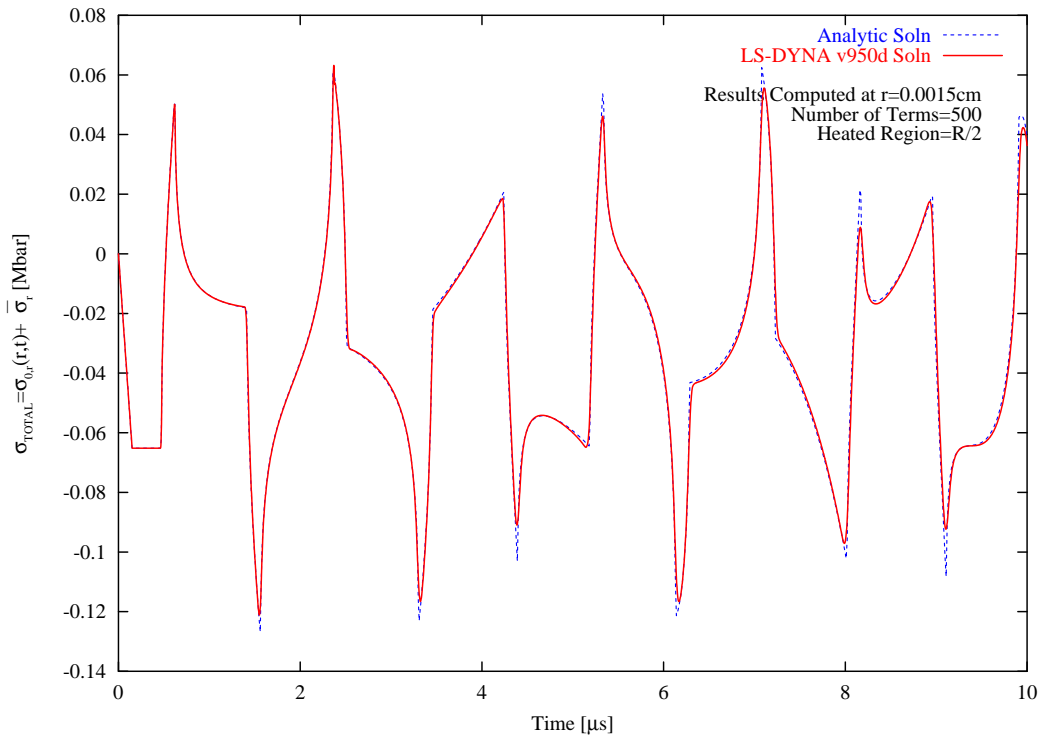

FIGURE 8. Comparison of the analytic vs. computational radial stress component during the period 40-50 μs for the case of a uniformly and instantaneously heated cylindrical rod.
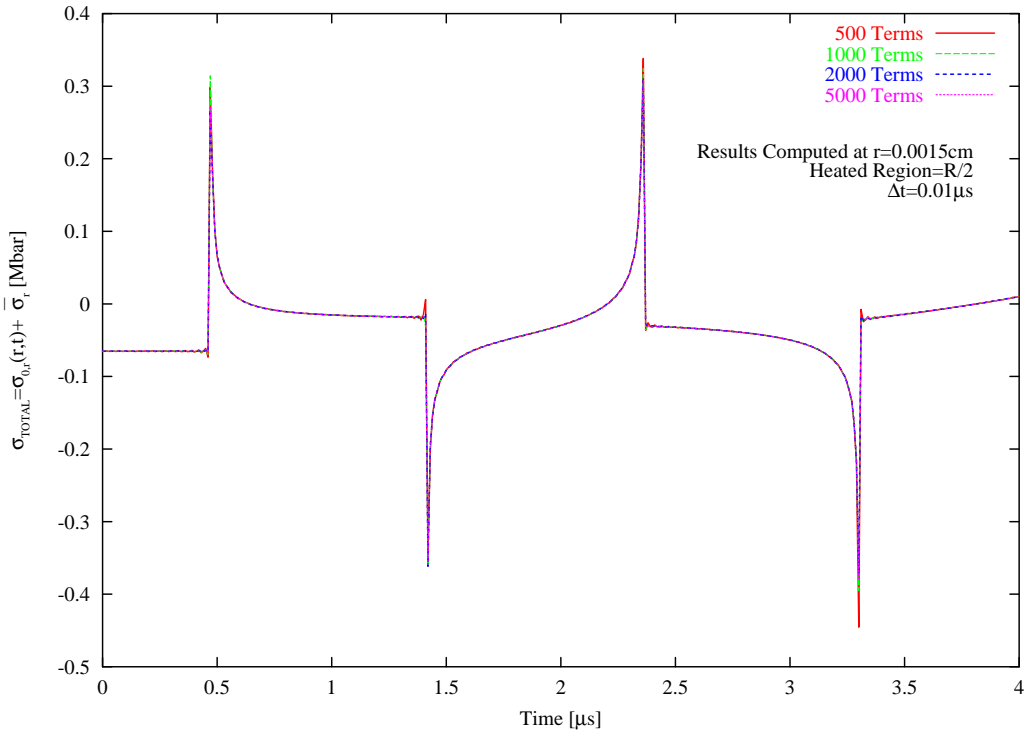
FIGURE 9. Parametric study of the number of terms used in the infinite series of the dynamic stress component of the total stress for the analytic solution.

FIGURE 10. Parametric study of the time increment, Δt, used in calculating the radial dynamic stress component of total stress for the analytic solution.
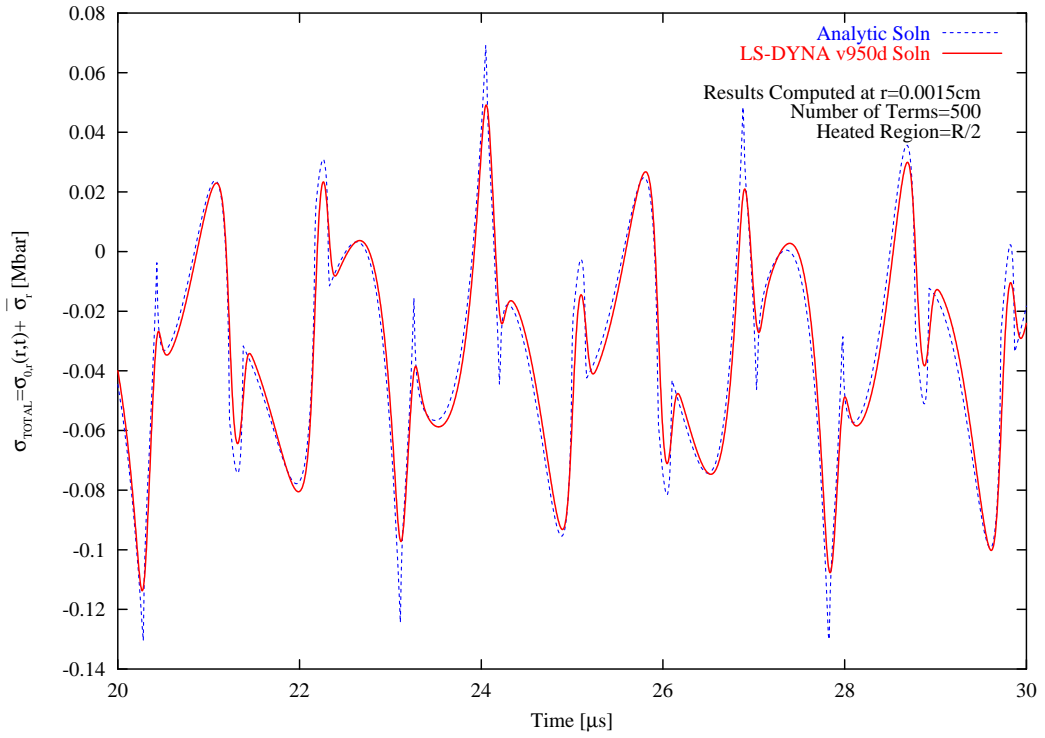
**FIGURE 11. Expanded view of Figure 13 for the time range 0.4-0.58 μs.**

FIGURE 12. Comparison of analytic vs. computational results for the radial stress component of a uniform, ramped thermal loading on a cylindrical rod of radius, R, and heated region, R/2. Five hundred terms of the infinite series for the dynamic component of "total" stress were used in the computation.

23

FIGURE 13. Comparison of radial stress component for the case of a uniform, ramped thermal loading over the period 20-30 μs on a cylindrical rod of radius R.
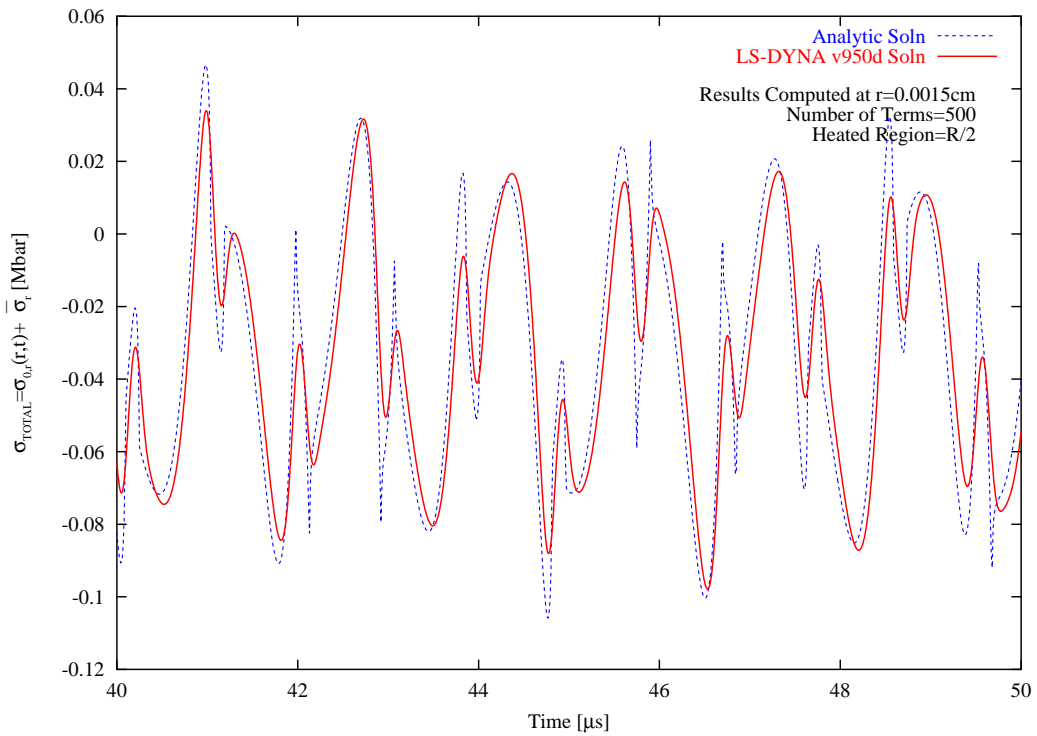
FIGURE 14. Comparison of radial stress component for the case of a uniform, ramped thermal loading over the period 40-50 μs on a cylindrical rod of radius R.